Available at www.sciencedirect.com

ScienceDirect

journal homepage: www.elsevier.com/locate/he

Hydrogen evolution reaction of low carbon steel electrode in hydrochloric acid as a source for hydrogen production

A.A. El-Meligi, N. Ismail*

National Research Centre, Physical Chemistry Department, Dokki, Cario, PO Box 12622, Egypt

ARTICLE INFO

Article history:
Received 21 September 2008
Received in revised form
8 October 2008
Accepted 9 October 2008
Available online 20 November 2008

Keywords:
Low carbon steel
Hydrochloric acid
Hydrogen evolution reaction
Hydrogen production
X-ray diffraction

ABSTRACT

The hydrogen evolution reaction (HER) (cathodic reaction) of low carbon steel electrode immersed in hydrochloric acid was investigated as a source for hydrogen production. Corrosion rate, hydrogen evolution rate, and current density increase with the increase of HCl concentration. Theoretically and practically, every 1 g of iron produces about 0.036 g of hydrogen. Therefore, the hydrogen production efficiency over the immersion period is about 100%. High correlation coefficient (close to +1) statistically indicates that there is a strong relation between loss in weight and the amount of evolved hydrogen (as dependent variable) and both time of immersion and acid concentrations (as independent variables). Application of the hydrogen produced by low carbon steel electrode has been performed on storage material. The tested material absorbs about 6 wt.% of hydrogen under atmospheric pressure and room temperature.

1. Introduction

Hydrogen is the future fuel because of its high heat of combustion- and high-energy capacity per unit volume as compared to oil and petroleum. The combustion products of hydrogen are nearly free from pollution. It was mentioned that hydrogen is the best fuel, particularly for transportation based on the following criteria: versatility, utilization efficiency and safety [1]. In fact, there are many attempts to use different electrodes for the hydrogen evolution reaction [2–7]. There is no attempt to use the as received carbon steel as a direct electrode for hydrogen production. It is only used as a substrate. For example, electrodes constructed with different electroactive materials such as platinum (Pt), nickel (Ni), 304 stainless steel (SS) and low carbon steel (LCS) have been tested in water electrolysis for hydrogen production [8]. The results showed that LCS electrode gave the highest current density and highest efficiencies production of high purity hydrogen by water electrolysis reaction. Also, carbon steel was used as a substrate for the deposition of composite Ni + Ti, Ni + V and Ni + Mo coatings which prepared by codeposition of Ti, V or Mo particles in nickel bath to form electrode for hydrogen production [9]. The modern industrial cathodes for the hydrogen evolution reaction (HER) are ferrous and nickel, which have higher hydrogen evolution overpotential of 380 and 480 mV, respectively, leading to greater consumption of electrical energy. Therefore, in recent years, numerous investigations have focused on the preparation of new electrode materials with high electrocatalytic activity for the HER [10–12]. Also, hydrogen can be produced by direct water splitting using photoelectrochemical (PEC) systems. Nanooxides, such as α-Fe_2O_3, can be used as suitable candidate for photoelectrochemical (PEC) splitting of water to generate hydrogen [13]. Other semiconductors oxides, such as TiO_2, WO_3, ZnO, $SrTiO_3$, Fe_2O_3, Cu_2O, SiO_2, etc., have been studied as photoelectrode in PEC cell for water splitting to

* *Corresponding author*. Tel.: +20 2 33733635; fax: +20 2 33370931.
E-mail address: ael_meligi10@hotmail.com (A.A. El-Meligi).

0360-3199/$ – see front matter
doi:10.1016/j.ijhydene.2008.10.026

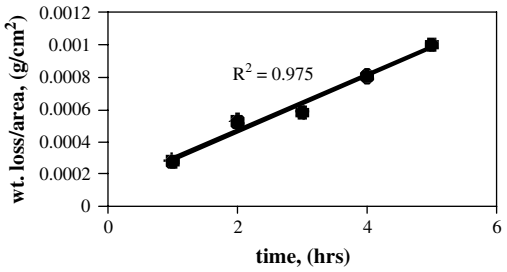

Fig. 1 – Corrosion trend of C1010 alloy immersed in 10% HCl at RT.

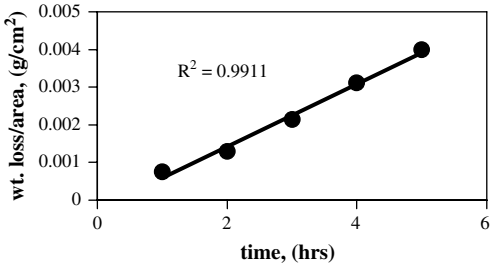

Fig. 3 – Corrosion trend of C1010 alloy immersed in 30% HCl at RT.

generate hydrogen [14–16]. In fact, there are limited attempts to use iron or carbon steel electrodes for the hydrogen production, especially, as substrate. For example, it is stated that the continuous oxidation of scrap iron in the presence of a constant CO_2-rich waste gas stream and water is evaluated as a means of sequestering anthropogenic CO_2 as well as generating hydrogen gas and electricity [17]. The main cathodic reaction for iron corroding in dilute inorganic acids is the reduction of hydrogen ions into hydrogen molecule (hydrogen evolution reaction (HER)) [18]. It was mentioned that hydrogen evolution reaction (HER) involves three reaction steps, Volmer (electrosorption), Heyrovsky (electrodesorption) and Tafel (recombination) [19]. The following suggested mechanisms: electrochemical discharge ($H^+ + e + M \rightarrow (M–H)$), recombination ($(M–H) + (M–H) \rightarrow 2M + H_2\uparrow$), and electrochemical desorption ($(M–H) + H^+ + e \rightarrow M + H_2\uparrow$) on the metal surface (M). Further, these mechanisms are said to be associated with the following likely reaction paths for hydrogen evolution reactions identified as: recombination reaction (path1) ($2H^+ + 2e \rightarrow 2H_{ads} \rightarrow H_2$), and the catalytic recombination (path 2) ($H^+ + e \rightarrow H_{ads} + H^+ + e \rightarrow H_2$) according to DeLuccia [20].

This work is mainly concerned with investigating the hydrogen evolution reaction (cathodic reaction) of the low carbon steel immersed in hydrochloric acid as a source for pure hydrogen production.

2. Experimental

2.1. Materials and electrolyte

Low carbon steel sheets (C1010) were used. The Q-Panel Company, European Branch Office, UK, provided the sample.

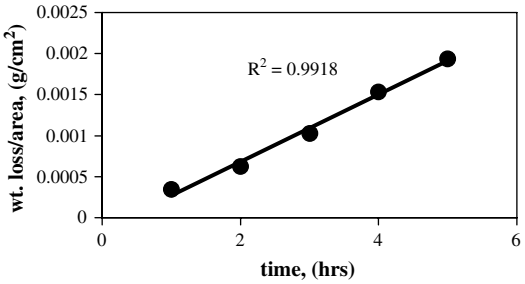

Fig. 2 – Corrosion trend of C1010 alloy immersed in 20% HCl at RT.

It is cold rolled. The sample composition is, C: 0.08–0.13%, Mn: 0.3–0.6%, P: 0.04%, S: 0.05% and Fe is the remaining.

The electrolyte is 10, 20 and 30% of hydrochloric acid solutions.

2.2. Experimental procedures

Low carbon steel sheets with an area of 10 cm^2 were used to run experiments. They were polished with different emery papers up to 1200 grade, washed with distilled water and degreased with acetone. The sheets were precisely weighed before and after immersing in 250 ml of 10–30% HCl solution.

Open circuit potential is processed on low carbon steel sheets immersed in different concentrations of HCl. Polarization measurements were operated after the specimen attained steady state potential. The polarization was carried out under scan rate of 10 mV/10 s in the cathodic direction. Low carbon steel sheet of an area 1 cm^2 is used as working electrode. Saturated calomel electrode (SCE), and platinum electrode are used as reference and counter electrodes, respectively. Potentiostat model 553 AMEL is used to run the experiments.

Scanning electron microscope (SEM) was performed to show topography of the alloy surface. The images were analyzed using a XL30 ESEM, high-vacuum mode. The acceleration voltage was 15 KV.

Microscopical examination of the low carbon steel alloy was operated using an optical microscope. It is Standard Olympus CH Microscope with Trinoclar head to which is fitted a CCTV (1/2) Video Camera. The Y/C (S-VHS) output is taken to an S-VHS Video Recorder and a Mitsubishi Color Video Printer, with the final signal being displayed on a 14 Sony Color Monitor.

X-ray diffraction (XRD) was carried out before and after immersion to define the crystal structure of the low carbon steel. The XRD patterns were recorded on a Siemens-D5000 diffractometer using Cu(kα) radiation ($\lambda = 0.15418$ nm). The X-ray tube was operated at 40 kV and 40 mA.

3. Results and discussion

3.1. Hydrogen evolution rate

Figs. 1–3 represent the relation between weight loss of low carbon steel (LCS) and immersion time in presence of 10%, 20%

Table 1 – The amount of iron and hydrogen estimated during immersion of low carbon steel in 10% HCl at RT.

time (h)	Amount of Fe $\times 10^{-4}$ (g)	Amount of $H_2 \times 10^{-4}$ (g)	Theoretically, 1 g of Fe produces 0.036 g H_2
			Practically, 1 g of Fe produces:
1	3.15	0.1125	0.035714
2	5.7	0.203571	0.035714
3	7.5	0.267857	0.035714
4	9	0.321429	0.035714
5	11.5	0.410714	0.035714

and 30% of HCl at room temperature (RT), respectively. As observed, the weight loss is increased with increasing HCl concentrations. This indicates that there is a regular loss in weight as a result of uniform behavior of the LCS. Consequently, the amount of hydrogen evolved is increased with increasing the HCl concentrations. Accordingly, the rate of corrosion and rate of hydrogen evolution are increased. As stated, the amounts of hydrogen evolved by the cathodic reaction are proportional to the corroded amounts of iron [18,21]. The number of hydrogen atoms released at the cathode equal the number of metal atoms oxidized at the anode multiplied by the number of electrons lost by each atom. The increase of the corrosion rate and rate of hydrogen evolution can be rationalized on the basis that HCl reacts with iron and forms metal chlorides, which are extremely soluble in aqueous media. The solubility of chloride salts does not hamper the rate of reaction [21,22]. There are two reactions occur the anodic reaction and cathodic reaction. The following equations represent iron reaction in acidic chloride solutions:

Anodic reaction (Oxidation reaction)

$$Fe \rightarrow Fe^{2+} + 2e \quad (1)$$

Cathodic (Reduction reaction or hydrogen evolution reaction)

$$2H^{+} + 2e \rightarrow H_2\uparrow \quad (2)$$

As calculated, rate of LCS alloy corrosion in 10% HCl is estimated 2×10^{-4} g cm^2 h^{-1}, in 20% HCl is 4×10^{-4} g cm^{-2} h^{-1} and in 30% HCl is 8×10^{-4} g cm^{-2} h^{-1}. Based on the following Equation (3), the rate of hydrogen evolved is estimated. The rate of hydrogen evolution of low carbon steel electrode in 10% HCl is 0.07143×10^{-4} g cm^{-2} h^{-1}, in 20% HCl is 0.14286×10^{-4} g cm^{-2} h^{-1}, and in 30% HCl is 0.2857×10^{-4} g cm^{-2} h^{-1}

$$M = [\underline{M} \times m(\text{atomic mass of metal})]/n \quad (3)$$

where M represents the mass of metal corroded or rate of corrosion, $\underline{M}$ the hydrogen amount or the rate of hydrogen evolution, n the number of electrons lost, and m is the atomic mass of iron. Practically, every one gram of iron produces 0.0357 g of hydrogen, as in Table 1. This result is coincidence with the theoretical one, in which, every one gram of Fe produces about 0.036 g of hydrogen and that one g of H_2 gas occupies 11200 cm^3 at 0 °C and at standard atmospheric pressure. Accordingly, the efficiency of the process (η) was calculated as the ratio between the amount of hydrogen produced and the amount of hydrogen theoretically produced [8], as shown by the Equation (4):

$$\eta\% = \left(\frac{M_{H_2}}{M^{\circ}_{H_2}}\right)100 \quad (4)$$

where M_{H_2} is the amount of hydrogen practically measured, and $M^{\circ}_{H_2}$ is the amount of hydrogen theoretically calculated. The hydrogen production efficiency over the period of immersion (1–5 h) in HCl is about 100%.

High correlation coefficients (R^2) are obtained from the relation between weight loss per unit area and immersion time. As in Figs. 1–3, the R^2 is equal 0.975 in presence of 10% HCl, R^2 is equal to 0.9918 in presence of 20% HCl and R^2 is 0.9911 in presence of 30% HCl at RT. These values are close to +1 indicating that there is a strong relation between weight loss (as independent variable) and dependent variables, such

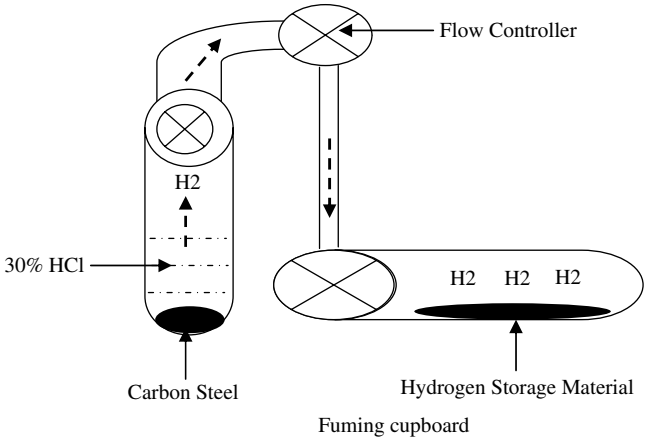

Fig. 4 – Schematic Diagram of the hydrogen production system. Sample of low carbon steel is immersed in 10% HCl at room temperature in a evacuated fuming cupboard under atmospheric pressure. Hydrogen is evolved and passed over the hydrogen storage material.

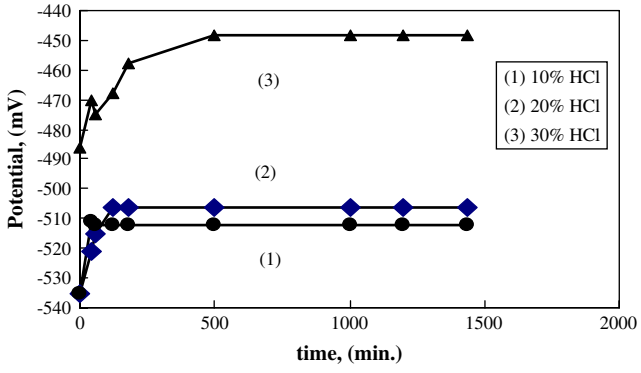

Fig. 5 – Open circuit potential of low C-steel in HCl at RT.

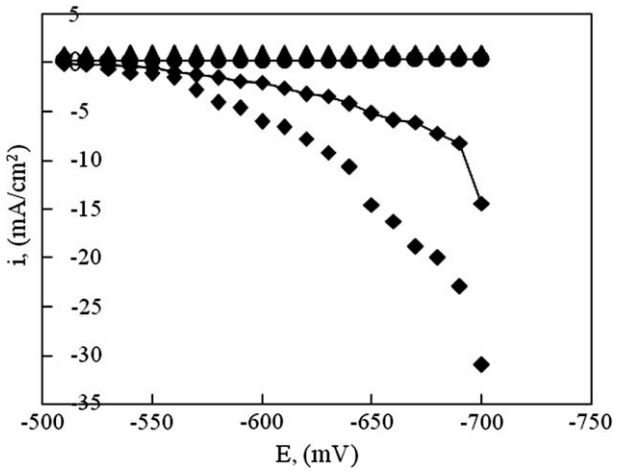

Fig. 6 – Potentiostatic polarization of low C-steel in HCl at RT.

as immersion time and acid concentrations [23]. Positive sign of the R^2 means that there is a linear increment of the weight loss. This means that the amount of hydrogen produced is directly proportional with increasing HCl concentrations.

The application of hydrogen production using the as received electrode of low carbon steel has been already preformed. The hydrogen production schematic system is as shown in Fig. 4. Hydrogen storage material was placed in the glass cell. The weight of hydrogen storage material before hydrogenation was 1.007 g. Hydrogen production was carried out via chemical reaction of low carbon steel electrode immersed in 100 ml of 30% HCl. The hydrogen was passed over the hydrogen storage material for 22 h under atmospheric pressure. After that, the sample was re-weighed and the weight was found to be 1.0707 g. The amount of hydrogen absorbed is $= 1.0707 - 1.007 = 0.0637$ g

Accordingly, the percent of hydrogen absorbed by the storage material is $= 0.0637/1.007 \times 100 = 6.33$ wt.%. This experiment has been repeated four times and gave almost the same results with ± 0.04 wt.% accuracy.

3.2. *Electrochemical behavior of LCS electrode*

The open circuit potential measurements of LCS electrode indicate that there is a shift to anodic direction with increasing the HCl concentrations, as in Fig. 5. It may be due to uniform formation of the temporary corrosion products. It was stated that the corrosion rate of iron and steel at room temperature in nitric acid decreases with increasing concentration above about 35% because of the formation of a passive oxide film on the metal surface. However, this passive condition is not completely stable [18]. As seen in Fig. 6, the

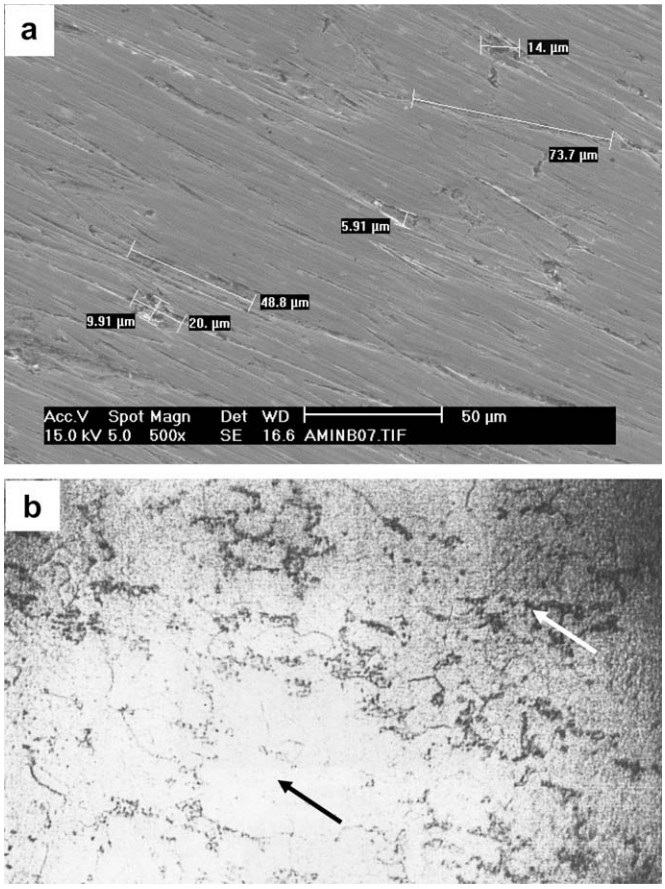

Fig. 7 – (a,b) Scanning electron detector photomicrograph of the as received low carbon steel alloy (a) and (b) is optical microscope examination of microstructure of low carbon steel alloy (black arrow refers to ferrite and white arrow refers to pearlite.

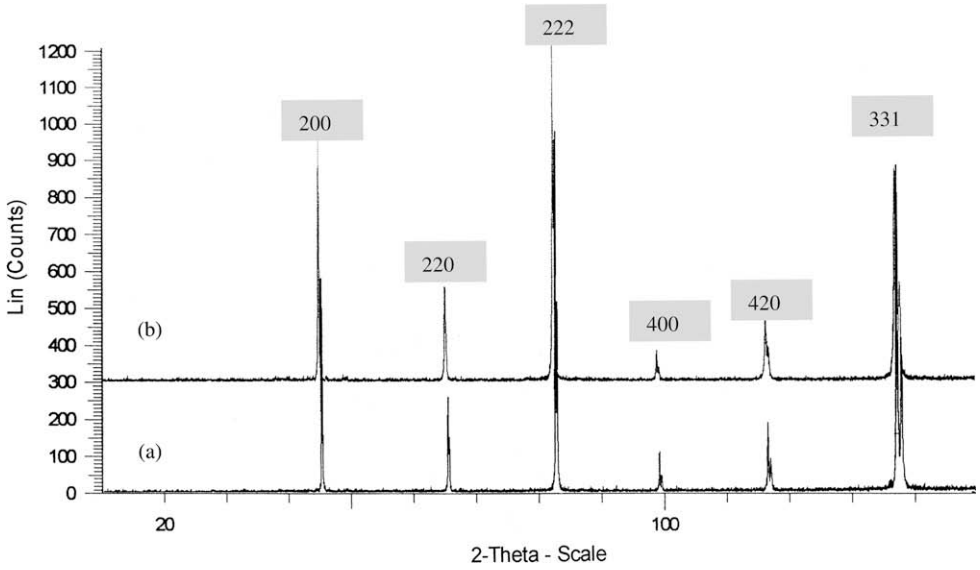

Fig. 8 – XRD patterns of C1010 alloy immersed for few hours in 30% HCl at: (a) RT and (b) 70 °C.

current density is enhanced with increasing the hydrochloric acid concentrations. The current density is about 5 mA/cm^2 in case of 10% HCl and is about 10 mA/cm^2 in case of 20% HCl. The current density increases with increasing HCl concentration. This means that the rate of hydrogen production is increased. These results are coincidence with results obtained of the low carbon steel electrode used to produce hydrogen of water electrolysis and it gave the highest current density and the highest efficiency of hydrogen production [8]. The potential where the hydrogen evolution reaction (HER) occurs is in the potential range of −550 to −700 mV. It was discussed that displacing the reduction potential to more cathodic values increases the current densities of the electrodes used for hydrogen production. Also, the values of current density depend strongly on the electrode material. The maximum current density observed for the low carbon steel (LCS) electrode and the current density observed for the stainless steel (SS) electrode is lower than of the LCS [8]. The presence of metals such as Ni, Cr and Mn in the composition of SS should be responsible for the low catalytic activity of this electrode in HER. This low catalytic activity is probably associated with the well-known passivation of SS in aqueous solutions [24].

3.3. *Surface morphology*

The photomicrograph (Fig. 7a) of the as-received alloy shows imperfectness of the surface. There are many defects and pores in the alloy matrix, which have different dimensions. Although the alloy has non-uniform surface, the corrosion behavior is uniform. It can be proposed that ionization of crystal phases occurs whether the surface is uniform or non-uniform. Surface imperfectness has no effect on uniformity behavior of corrosion process. Consequently, the hydrogen evolution reaction (HER) is distributed over the whole surface. The imperfectness of the alloy surface informs the presence of huge number of anodic and cathodic areas on the alloy surface. As discussed [21], the

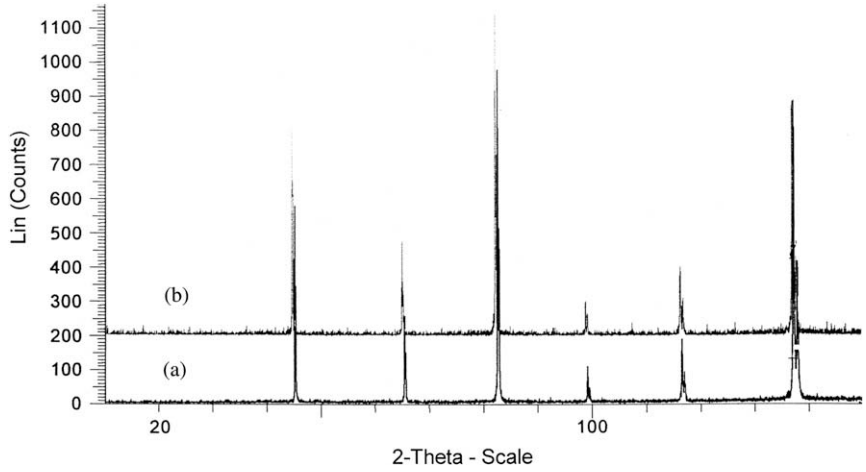

Fig. 9 – XRD patterns of C1010 alloy immersed for few hours in: (a) 20% HCl at 70 °C and (b) 30% HCl at 70 °C.

anodic and cathodic areas may shift from time to time so as to give the appearance of uniform corrosion of mild steel placed in hydrochloric acid. These areas, however, are often so small to be invisible and so numerous to be almost inseparable. Accordingly, the hydrogen evolution reaction will be numerous and it can be proposed that hydrogen will be generated in a continuous stream and can be collected to be charged into storage materials. The main constituent of the low carbon steel alloy is ferrite [21]. As shown in Fig. 7b of microscopical examination by optical microscope, all clear areas represent the ferrite structure. Areas of moderately coarse pearlite are arranged in a background of ferrite. It is stated that the microstructure of low carbon steel and weathering steel affects their corrosion behavior [25]. Consequently, the hydrogen evolution reaction will be affected.

3.4. *X-ray diffraction and hydrogen evolution*

As seen in Figs. 8 and 9, the X-ray diffraction (XRD) patterns of the C1010 alloy were recorded after immersing in 10–30% of HCl at different temperatures. It is observed that the alloy structure is well crystalline, even under drastic conditions of 20–30% of HCl and high temperature of 70 °C. The patterns are indexed on the cubic unit cell for the iron *hkl* phases as presented in the Table 2. It is evidenced from the patterns that there is no significant change in the *hkl* phases of the alloy in presence of different HCl concentrations at different temperatures. The *hkl* phases have different atomic density and these atoms de-ionize from the crystal lattice [26,27]. Therefore, it can be proposed that there is a uniform ionization of the crystal *hkl* phases leading to uniform corrosion. Accordingly, hydrogen evolution reaction occurs uniformly over the whole surface. This can lead to continuous stream of hydrogen, which can be collected for application. The crystal structure is formed of different *hkl* phases (Table 2).

The crystal planes produce unit cells of various shapes, depending on how these planes are arranged [28]. In case of cubic unit cell, the planes sets are equally spaced and mutually perpendicular (i.e. the lattices parameters, $a = b = c$ and the angles $\alpha = \beta = \gamma = 90^{\circ}$). The cubic cell has the advantages overall the other unit cells where all lattices points of the body are located at equal distances from the center [29]. The cubic advantages and its symmetry may be considered one of the key points to explain the corrosion behavior of the steel. It can be proposed that uniform ionization of the Fe atoms may occur. Consequently, a continuous stream of hydrogen will be produced.

Table 2 – The lattice parameters and *hkl* phases of the Fe cubic structure.

Unit cell is cubic and the lattice parameters, $a = b = c = 4.05566$ Å and $\alpha = \beta = \gamma = 90^{\circ}$

Fe phases	*hkl* values	*d*-spacing between phases (Å)	Bragg's angles
Phase 1	111	2.34154	38.4127
Phase 2	200	2.02783	44.65042
Phase 3	220	1.43389	64.9875
Phase 4	311	1.22283	78.09018
Phase 5	222	1.17077	82.28626
Phase 6	400	1.01392	98.88016
Phase 7	420	0.90687	116.29292
Phase 8	331	0.93043	111.76572

4. Conclusion

Cathodic reaction (hydrogen evolution reaction (HER)) of carbon steel in hydrochloric acid is important as a source for hydrogen. The corrosion rate is increased with increasing concentrations of HCl. Consequently, the rate of hydrogen evolved is increased. High correlation coefficient is obtained and it has a positive sign. This means that there is a strong correlation between the loss in weight loss and amount of evolved hydrogen (as dependent variable) and dependent variables (the immersion time, acid concentrations and temperature). The open circuit potential shifts to anodic direction with increasing the HCl concentrations. The crystal structure of the alloy is indexed on a cubic unit cell. The cubic advantages overall the other unit cells as it is coincidence with itself and has the highest symmetry among them. Accordingly, regular ionizations of iron atoms may occur of crystal planes (*hkl* phases). This regularity may lead to a uniform corrosion. Consequently, a uniform distribution of the hydrogen evolution reaction will occur and leads to continuous stream of hydrogen. The hydrogen can be easily collected by passing over hydrogen storage material. This experiment has already been done and the hydrogen storage material absorbed about 60 g H_2/kg of the material. The work is under preparation to be published.

REFERENCES

[1] Veziroglu TN, Barbir F. Tranportation fuel-hydrogen. In: Energy technology and the environment, vol. 4. New York: Wiley; 1995. p. 2712–30.
[2] Shan Z, Liu Y, Chen Z, Warrender G, Tian J. Amorphous Ni–S–Mn alloy as hydrogen evolution reaction cathode in alkaline medium. International Journal of Hydrogen Energy 2008;33:28–33.
[3] De Giz MJ, Tremiliosi-Filho G, Gonzalez ER, Srinivasan S, Appleby AJ. The hydrogen evolution reaction on amorphous nickel and cobalt alloys. International Journal of Hydrogen Energy 1995;20(6):423–7.
[4] Wang Y, Lu ZW, Gao XP, Hu WK, Jiang XY, Qu JQ, et al. Electrochemical properties of the ball-milled $LaMg_{10}Ni_2$–xAl_x alloys with Ni powders (x = 0, 0.5, 1 and 1.5). Journal of Alloys and Compounds 2005;389(1–2):290–5.
[5] Arul RI. Nickel-based, binary-composite eletrocatalysts for the cathodes in the energy-efficient industrial production of hydrogen from alkaline water electrolytic cells. Journal of Applied Electrochecmistry 2000;30(5):499–504.
[6] Qing H, Huiren L, Jianshe C, Xujun W. A study of the electrodeposited Ni–S alloys as hydrogen evolution reaction cathodes. International Journal of Hydrogen Energy 2003;28(11):1207–12.
[7] Qing H, Huiren L, Jianshe C, Xin L, Xujun W. Study of amorphous Ni–S–Co alloy used as hydrogen evolution reaction cathode in alkaline medium. International Journal of Hydrogen Energy 2004;29:243–8.

[8] de Souza Roberto F, Padilha Janine C, Gonçalves Reinaldo S, de Souza Michele O, Rault-Berthelot Joëlle. Electrochemical hydrogen production from water electrolysis using ionic liquid as electrolytes: towards the best device. Journal of Power Sources 2007;164(2):792–8.
[9] Panek Joanna, Budniok Antoni. Production and electrochemical characterization of Ni-based composite coatings containing titanium, vanadium or molybdenum powders. Surface and Coatings Technology 2007;201(14):6478–83.
[10] Rosalbino F, Maccio D, Angelini E, Saccone A, Delfino S. Electrocatalytic properties of Fe–R (R = rare earth metal) crystalline alloys as hydrogen electrodes in alkaline water electrolysis. Journal of Alloys and Compounds 2005;403(1–2): 275–82.
[11] Metikos-Hukovic M, Grubac Z, Radic N, Tonejc A. Sputter deposited nanocrystalline Ni and Ni–W films as catalysts for hydrogen evolution. Journal of Molecular Catalysis A: Chemical 2006;249(1–2):172–80.
[12] Hu WK. Electrocatalytic properties of new electrocatalysts for hydrogen evolution in alkaline water electrolysis. International Journal of Hydrogen Energy 2000;25(2):111–8.
[13] Satsangia Vibha R, Kumaria Saroj, Singha Aadesh P, Shrivastavb Rohit, Dass Sahab. Nanostructured hematite for photoelectrochemical generation of hydrogen. International Journal of Hydrogen Energy 2008;33(1):312–8.
[14] Björksten U, Moser J, Grätzel M. Photoelectrochemical studies on nanocrystalline hematite films. Chemistry of Materials 1994;6(6):858.
[15] Zaban A, Aruna ST, Tirosh S, Gregg BA, Mastai Y. The effect of the preparation condition of TiO_2 colloids on their surface structures. The Journal of Physical Chemistry B 2000;104(17): 4130.
[16] Aroutiounian VM, Arakelyan VM, Shahnazaryan GE. Metal oxide photoelectrodes for hydrogen generation using solar radiation-driven water splitting. Solar Energy 2005;78(5):581.
[17] Rau Greg H. Possible use of Fe/CO_2 fuel cells for CO_2 mitigation plus H_2 and electricity production. Energy Conversion and Management 2004;45(13–14):2143–52.
[18] Roberge PR. Corrosion engineering: principles and practice. McGrow Hill; March 30, 2008.
[19] Harrington DA, Conway BE. AC impedance of faradaic reactions involving electrosorbed intermediates—I. Kinetic theory. Electrochimica Acta 1987;32(12):1703.
[20] DeLuccia John J. Electrochemical aspects of hydrogen in metals. ASTM STP 962. In: Raymond L, editor. Hydrogen embrittlement: prevention and control. Philadelphia: American Society for Testing and Materials; 1988. p. 17–34.
[21] National Association of Corrosion Engineers (NACE). ''Corrosion Basics'' an introduction; 1984. 30.
[22] El-Meligi AA. PhD thesis, UMIST and Cairo University; 1999. p. 3.
[23] Rice JA. Mathematical statistics and data analysis. 2nd ed. Belmont: Wadsworth Publishing Company; 1995.
[24] Wang XY, Li DY. Beneficial effects of yttrium on the mechanical failure and chemical stability of the passive film of 304 stainless steel. Materials Science and Engineering 2001;315(1–2):158–65.
[25] Higgins RA. Engineering metallurgy, part I, applied physical metallurgy. p. 67. [Chapter IV].
[26] Chiba M, Seo M. Effects of dichromate treatment on mechanical properties of passivated single crystal iron (1 0 0) and (1 1 0) surfaces. Corrosion Science 2002;44(10): 2379–91.
[27] Chiba M, Seo M. Mechanoelectrochemical properties of passive iron surfaces evaluated by an *in situ* nanoscratching test. Journal of the Electrochemical Society 2003;150(11): B525–9.
[28] Cheetham AK, Day P. Solid state chemistry techniques. Oxford Univ. Press; 1987.
[29] Cullity BD. Elements of X-ray diffraction. 2nd ed.; 1978.